# The Human CXC Chemokine Granulocyte Chemotactic Protein 2 (GCP-2)/CXCL6 Possesses Membrane-Disrupting Properties and Is Antibacterial[▽]

Helena M. Linge,[1*] Mattias Collin,[1] Pontus Nordenfelt,[1] Matthias Mörgelin,[1] Martin Malmsten,[2] and Arne Egesten[3]

Divisions of Infection[1] and Respiratory[3] Medicine, Department of Clinical Sciences Lund, Lund University, SE-221 84 Lund, and Department of Pharmacy, Uppsala University, SE-751 23 Uppsala,[2] Sweden

Granulocyte chemotactic protein 2 (GCP-2)/CXCL6 is a CXC chemokine expressed by macrophages and epithelial and mesenchymal cells during inflammation. Through binding and activation of its receptors (CXCR1 and CXCR2), it exerts neutrophil-activating and angiogenic activities. Here we show that GCP-2/CXCL6 itself is antibacterial. Antibacterial activity against gram-positive and gram-negative pathogenic bacteria of relevance to mucosal infections was seen at submicromolar concentrations (minimal bactericidal concentration at which 50% of strains tested were killed, $0.063 \pm 0.01$ to $0.37 \pm 0.03$ μM). In killed bacteria, GCP-2/CXCL6 associated with bacterial surfaces, which showed membrane disruption and leakage. A structural prediction indicated the presence of three antiparallel $NH_2$-terminal β-sheets and a short amphipathic COOH-terminal α-helix; the latter feature is typical of antimicrobial peptides. However, when the synthetic derivatives corresponding to the $NH_2$-terminal (50 amino acids) and COOH-terminal (19 amino acids, corresponding to the putative α-helix) regions were compared, higher antibacterial activity was observed for the $NH_2$-terminus-derived peptide, indicating that the holopeptide is necessary for full antibacterial activity. An artificial model of bacterial membranes confirmed these findings. The helical content of GCP-2/CXCL6 in the presence or absence of lipopolysaccharide or negatively charged membranes was studied by circular dichroism. As with many antibacterial peptides, membrane disruption by GCP-2/CXCL6 was dose-dependently reduced in the presence of NaCl, which, we here demonstrate, inhibited the binding of the peptide to the bacterial surface. Compared with CXC chemokines ENA-78/CXCL5 and NAP-2/CXCL7, GCP-2/CXCL6 showed a 90-fold-higher antibacterial activity. Taken together, GCP/CXCL6, in addition to its chemotactic and angiogenic properties, is likely to contribute to direct antibacterial activity during localized infection.

---

Chemokines are a family of peptides containing conserved cysteine motifs in their $NH_2$ terminus, i.e., XC, CC, CXC, and $CX_3C$, where "X" is a nonconserved amino acid residue (1). These molecules are responsible for leukocyte trafficking and activation during both health and disease. Human granulocyte chemotactic protein 2 (GCP-2)/CXCL6 is an ELR-positive CXC chemokine with a length of 77 amino acids (18). The $NH_2$-terminal glutamic acid-leucine-arginine (ELR) motif is characteristic of CXC chemokines interacting with the G-protein-coupled receptors CXCR1 and CXCR2, which are expressed on a variety of cells, e.g., neutrophils, monocytes/macrophages, T and NK cells, mast cells, and endothelial cells (1, 26). In the case of leukocytes, GCP-2/CXCL6 binding to the receptors causes cellular activation, chemotaxis, and sometimes, depending on the context, execution of cytotoxic effector functions (1). Activation of endothelial cells by GCP-2/CXCL6 causes a mitogenic response, resulting in angiogenesis (10). GCP-2/CXCL2 is expressed by epithelial cells of the airways, eyes, gastrointestinal tract, mammary glands, tonsils, macrophages, and mesenchymal cells, in particular during inflammation (6, 10, 15–17, 22). Lipopolysaccharides (LPS) and the proinflammatory cytokines tumor necrosis factor alpha and interleukin-1β (IL-1β) up-regulate the expression of GCP-2/CXCL6, while gamma interferon has a down-regulating effect (27).

β-Defensins are potent antimicrobial peptides produced by inflamed epithelium (9). In recent years, some chemokines have been demonstrated to exert defensin-like antimicrobial activity. Examples of these are the CC chemokines macrophage inflammatory protein 3α/CCL20 and mucosa-associated epithelial chemokine/CCL28, as well as the ELR-negative CXC chemokine MIG/CXCL9 (4, 11, 29). Given that GCP-2/CXCL6 is expressed by epithelial cells at mucosal surfaces prone to infection, we investigated the potential antibacterial activity of this chemokine. In the present study, we show for the first time that GCP-2/CXCL6 disrupts membranes and is a potent antibacterial chemokine with activity against several bacterial pathogens relevant in mucosal infections.

## MATERIALS AND METHODS

**Chemicals and reagents.** Recombinant human chemokines GCP-2/CXCL6, epithelial-cell-derived neutrophil attractant 78 (ENA-78)/CXCL5, and neutrophil-activating peptide 2 (NAP-2)/CXCL7, affinity-purified polyclonal rabbit antibodies against GCP-2/CXCL6, and preimmune rabbit immunoglobulin G (IgG) were from PeproTech, London, United Kingdom. The synthetic peptides GPV-50 (GPVSAVLTEL RCTCLRVTLR VNPKTIGKLQ VFPAGPQCSK VEVVASLKNG) and APF-19 (APFLKKVIQK ILDSGNKKN), derived from the sequence of the mature human GCP-2/CXCL6 holopeptide, were 95% pure (Genscript Corporation, Piscataway, NJ). Citrated plasma from healthy donors was obtained from the Blood Center, University Hospital, Lund, Sweden.

* Corresponding author. Present address: Section for Cardiopulmonary Research, Feinstein Institute for Medical Research, 350 Community Drive, Manhasset, NY 11030. Phone: (516) 562-3464. Fax: (516) 562-1022. E-mail: hlinge@nshs.edu.

**Bacterial strains and growth conditions.** *Streptococcus pyogenes* strain AP1 (40/58), serotype M1, was from the World Health Organization Collaborating Centre for Reference and Research on Streptococci, Prague, Czech Republic. *Streptococcus dysgalactiae* subsp. *equisimilis* (strain G41), *Staphylococcus aureus* (strains 5120 and Newman), *Pseudomonas aeruginosa* (strain 1553), and *Escherichia coli* (strain 37.4) were obtained from the Division of Infection Medicine, Department of Clinical Sciences, Lund University, Lund, Sweden. Bacteria were routinely grown in Todd-Hewitt (TH; Difco/Becton Dickinson, Franklin Lakes, NJ) liquid medium under 5% $CO_2$ at 37°C. *Candida albicans* (strain 90028; ATCC, Manassas, VA) was grown in Sabouraud's dextrose broth (Difco).

**Bactericidal assay.** Bacteria were cultivated to mid-log phase (optical density at 620 nm, 0.4) in TH medium, washed, and diluted in incubation buffer (10 mM Tris-HCl containing 5 mM glucose [pH 7.4]). *P. aeruginosa* and *C. albican*s were grown for 18 h at 37°C, the latter with aeration to limit the formation of hyphae. Fifty microliters of bacteria ($10^6$ CFU/ml) was incubated together with various concentrations of peptide or buffer alone for 1 h at 37°C. To quantitate bactericidal activity, serial dilutions of the incubation mixtures were plated onto TH agar. Plates containing fewer than 30 or more than 200 CFU were excluded from the experiment. The mean minimal bactericidal concentration (MBC) for each species was calculated.

**Fluorescence labeling and microscopy.** *E. coli* ($10^7$ CFU/ml) was incubated with GCP-2/CXCL6 (1 μM) for 1 h and thereafter fixed in 4% paraformaldehyde (Sigma, St. Louis, MO) for 15 min at 37°C. The bacteria were then centrifuged for 10 min at 2,000 × g at room temperature, and the resulting pellet was resuspended in 100 μl affinity-purified rabbit anti-GCP-2/CXCL6 solution (2 μg/ml) containing 5% goat serum (Sigma) and incubated for 45 min at room temperature. Following a wash step in Tris-HCl (10 mM; pH 7.4) with 0.2% saponin, secondary goat anti-rabbit $F(ab')_2$ fragments (conjugated to Alexa 594; diluted 1:1,000; Invitrogen, Stockholm, Sweden) were added in a volume of 100 μl containing 5% goat serum. Samples were incubated for 30 min at room temperature. Following two wash steps, pellets were resuspended in 50 μl phosphate-buffered saline (PBS). The suspensions were added to ethanol-washed coverslips and allowed to sediment for 1 h at room temperature. Coverslips were mounted on glass slides (Super Frost; Menzel-Gläser, Braunschweig, Germany) using ProLong Gold Antifade reagent with 4′,6′-diamidino-2-phenylindole (DAPI) for visualization of DNA (Invitrogen). Images were acquired using a fluorescence microscope (Nikon Eclipse TE300 inverted microscope; Nikon Kogaku, Tokyo, Japan). A total of 446 bacteria from three different experiments were analyzed for enumeration purposes.

**Negative staining and transmission electron microscopy.** Bacteria were incubated with GCP-2/CXCL6 (1 μM) in incubation buffer for 1 h at 37°C. The specimens were subjected to negative staining using 0.75% uranyl formate as described elsewhere (21). Specimens were examined in a JEOL (Tokyo, Japan) 1200EX transmission electron microscope operated at 60 kV accelerating voltage.

**Molecular modeling.** A homology structure model of GCP-2/CXCL6 was constructed using the Swiss-Model automated homology modeling server (23) with connective-tissue-activating peptide III (PDB 1F9P) as the template. The model was visualized using the VMD (version 1.8.5) application (12). For helical wheel depiction, EMBOSS Pepwheel software (http://emboss.sourceforge.net /apps/release/4.0/emboss/apps/pepwheel.html) was used (20).

**Liposome preparation and leakage assay.** Dry lipid films were prepared by dissolving dioleoylphosphatidylethanolamine (1,2-dioleoyl-*sn-glycero*-3-phosphoethanolamine, >99% pure [DOPE]) (70 mol%) and dioleoylphosphatidylglycerol (1,2-dioleoyl-*sn-glycero*-3-phosphoglycerol, >99% pure [DOPG]) (30 mol%) (both from Avanti Polar Lipids, Alabaster, AL) and then removing the solvent by evaporation under a vacuum overnight. Subsequently, buffer (10 mM Tris [pH 7.4]) was added together with 0.1 M carboxyfluorescein (CF) (Sigma, St. Louis, MO). After hydration, the lipid mixture was subjected to eight freeze-thaw cycles consisting of freezing in liquid nitrogen and heating to 60°C. Unilamellar liposomes (diameter, ca. 140 nm) were generated by multiple extrusions through polycarbonate filters (pore size, 100 nm) mounted in a LipoFast miniextruder (Avestin, Ottawa, Ontario, Canada) at 22°C. Untrapped CF was then removed by two gel filtrations (Sephadex G-50) at 22°C, with Tris buffer as the eluent. CF release was determined by monitoring the fluorescence emitted at 520 nm from liposome dispersions (10 mM lipid in 10 mM Tris). An absolute leakage scale was obtained by disrupting the liposomes at the end of the experiment by addition of 0.8 mM Triton X-100 (Sigma, St. Louis, MO), causing 100% release and dequenching of CF. Throughout, a Spex Fluorolog 1650 0.22-m double spectrometer (Spex Industries, Edison, NJ) was used for the liposome leakage assay. Measurements were performed at 37°C.

**CD spectroscopy.** The circular dichroism (CD) spectra of the peptides in solution were measured on a J-810 spectropolarimeter (Jasco, United Kingdom). Measurements were performed at 37°C in a 10-mm quartz cuvette under stirring,

and the protein/peptide structure was monitored in the range of 200 to 260 nm. We subtracted the background value detected at 250 nm and corrected for signals from the bulk solution. The secondary structure was monitored at a peptide concentration of 10 μM in buffer alone, in the presence of liposomes (lipid concentration, 100 μM), and in the presence of LPS from *E. coli* 0111:B4 (0.2 mg/ml; Sigma-Aldrich, St. Louis, MO). The helix content was quantified at 222 to 225 nm by using reference spectra for samples containing 100% α-helix and 100% random coil. As references, we used 0.133 mM (monomer concentration) poly-L-lysine in 0.1 M NaOH and HCl, respectively.

**Western blot analysis for binding of GCP-2/CXCL6 to the bacterial surface.** *S. aureus* (strain Newman) bacteria were cultured overnight in 10 ml TH medium, pelleted by centrifugation, washed three times, and resuspended in 1 ml of 10 mM Tris-HCl (pH 7.5). Then 100 μl of bacteria was incubated for 5 min at room temperature with 5 μg of GCP-2/CXCL6 or human IgG (Sigma) in 100 μl of the same buffer with or without NaCl at a final concentration of 150 mM. Samples were washed three times with 1 ml of buffer with or without NaCl. Bacterial pellets were resuspended in 50 μl of sodium dodecyl sulfate-polyacrylamide gel electrophoresis (SDS-PAGE) sample buffer. Five microliters of sample was separated by SDS-PAGE (using 16.5% Tris-Tricine gels for GCP-2/CXCL6-incubated samples and 10% Tris-glycine gels for IgG-incubated samples), followed by electroblotting to polyvinylidene difluoride membranes (Immobilon-P; Millipore, Bedford, MA). The membrane containing GCP-2/CXCL6 was blocked with Superblock T20 (PBS) (Pierce, Rockford, IL), followed by incubation with polyclonal anti-GCP-2/CXCL6 antibodies (dilution, 1:1,000; Peprotech) in Superblock, a wash in PBS with 0.1% Tween 20 (PBST), incubation with horseradish peroxidase-conjugated goat anti-rabbit IgG (1:3,000; Bio-Rad, Hercules, CA) in Superblock, and a wash in PBST. The membrane containing IgG was blocked with PBST containing 5% (wt/vol) skim milk, followed by incubation with horseradish peroxidase-conjugated protein G (1:5,000; Bio-Rad) and a wash in PBST. Both membranes were developed using the SuperSignal West Pico peroxidase substrate (Pierce) and were analyzed using a Chemidoc XRS imaging system and Quantity One image analysis software (Bio-Rad).

## RESULTS

**GCP-2/CXCL6 possesses antibacterial activity.** GCP-2/CXCL6 was examined for potential antibacterial activity against a panel of bacteria relevant as causative agents of infections of dermis and mucosal surfaces. The bacteria included gram-positive (*S. pyogenes*, *S. dysgalactiae* subsp. *equisimilis*, and *S. aureus*) and gram-negative (*E. coli* and *P. aeruginosa*) bacteria. By use of a bactericidal assay, GCP-2/CXCL6 showed bactericidal effects against all bacterial species investigated. The concentrations killing 50% and 90% of the bacteria, respectively, are displayed in Table 1. GCP-2/CXCL6 at concentrations as high as 2 μM (16 μg/ml) did not affect the survival of *C. albicans*.

**GCP-2/CXCL6 associates with the surfaces of bacteria and evidently causes disruption of bacterial membranes.** To further investigate the interaction of GCP-2/CXCL6 with bacterial membranes, bacteria were subjected to the bactericidal

TABLE 1. GCP-2/CXCL6 is antibacterial toward both gram-positive and gram-negative bacterial pathogens[a]

| Species | MBC (μM)[b] | |
| --- | --- | --- |
| | 50% | 90% |
| *S. pyogenes* | 0.063 ± 0.01 | 0.30 ± 0.12 |
| *S. dysgalactiae* subsp. *equisimilis* | 0.087 ± 0.01 | 0.28 ± 0.06 |
| *S. aureus* | 0.30 ± 0.08 | 0.59 ± 0.15 |
| *E. coli* | 0.24 ± 0.03 | 0.46 ± 0.01 |
| *P. aeruginosa* | 0.37 ± 0.03 | 0.96 ± 0.04 |

[a] Bactericidal assays were performed using the indicated bacterial species, which were cultured to mid-log phase and then incubated with GCP-2/CXCL6 at increasing concentrations for 1 h at 37°C.
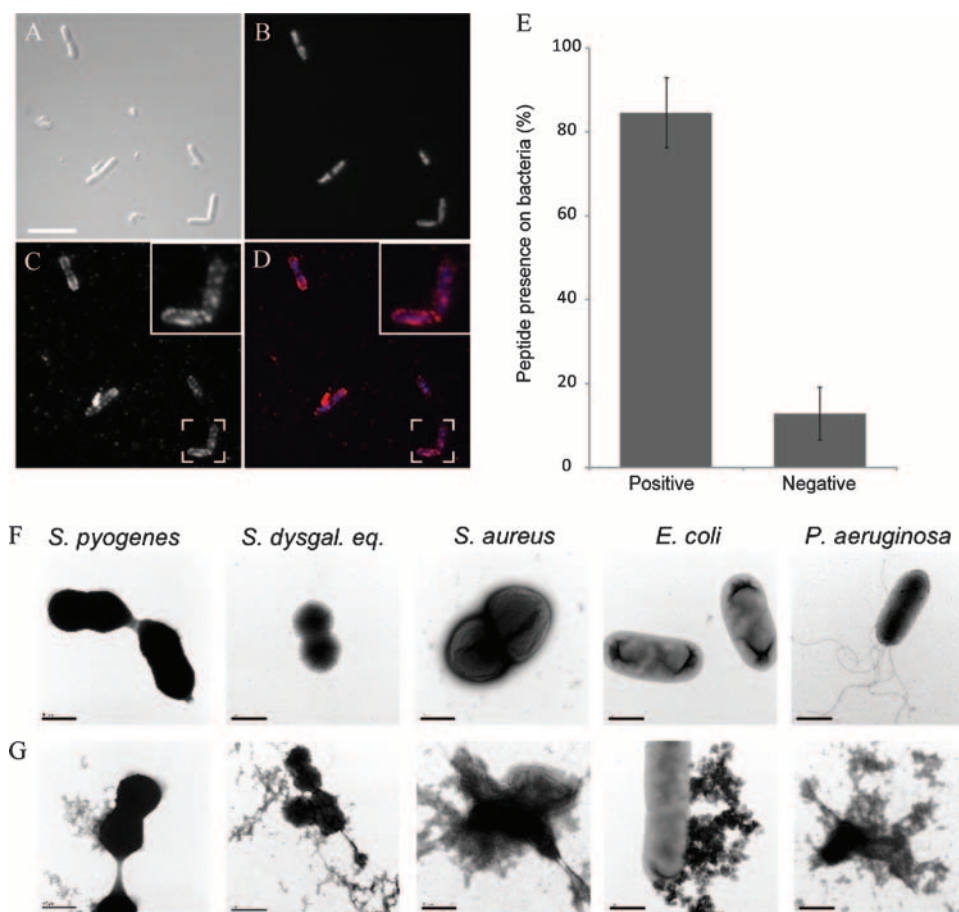
[b] Values are means ± SEM.

FIG. 1. GCP-2/CXCL6 associates with the bacterial surface and disrupts bacterial membranes. (A to D) *E. coli* was exposed to GCP-2/CXCL6 (1 μM) for 1 h at 37°C. After fixation, the bacteria were labeled and immobilized on glass slides. (A) Differential interference contrast image of the stained bacteria. (B) Bacterial DNA is visualized by binding of the fluorescent dye DAPI. (C) Immunolabeled GCP-2/CXCL6. (D) Merge composite of panels B and C, showing DNA in blue and immunolabeled GCP-2/CXCL6 in red. Results are representative of three separate experiments. Scale bar, 10 μm. (E) The stained bacteria were enumerated, and results are displayed in a bar graph. (F and G) Electron micrographs showing bacteria incubated in buffer alone (F) or with GCP-2/CXCL6 (1 μM) (G) for 1 h at 37°C, followed by negative staining. Bacteria exposed to GCP-2/CXCL6, but not control samples, show protrusions and leakage of intracellular contents. Scale bars, 0.5 μm.

assay and then immunolabeled to detect GCP-2/CXCL6 (Fig. 1). To avoid nonimmune binding of antibodies to bacterial surface proteins (e.g., protein A of staphylococci or protein G of streptococci), *E. coli* was chosen for these experiments. Bacteria are depicted by differential interference contrast (Fig. 1A), and the DNA is visualized, providing a perspective (Fig. 1B). The peptide staining pattern showed an intense "dot-like" appearance, as visualized by fluorescence microscopy (Fig. 1C and D). This suggests that GCP-2/CXCL6 may polymerize or accumulate before or during binding to the bacterial surface. The results from enumeration of positively and negatively stained bacteria showed that GCP-2/CXCL6 associated with approximately 80% of the bacteria (Fig. 1E).

Electron microscopy was used to visualize the effect of GCP-2/CXCL6 on the integrity of the bacteria during killing. In contrast to untreated control bacteria (Fig. 1F), bacteria incubated with GCP-2/CXCL6 showed membrane protrusions and leakage of cellular contents (Fig. 1G).

**Structural prediction and physiochemical properties of GCP-2/CXCL6 in relation to its antibacterial activity.** In order

to define the antibacterial region of GCP-2/CXCL6, a predictive model based on known structures of other members of the chemokine family was made (Fig. 2). GCP-2/CXCL6 contains the typical CXC motif that forms disulfide bonds with cysteines 12 to 38 and 14 to 54 (Fig. 2). The NH₂ terminus, most likely, is an unstructured region, followed by three antiparallel β-sheets and a short α-helix (Fig. 2A). When the amino acids are displayed by class (hydrophobic or hydrophilic), the α-helical COOH-terminal region shows amphipathic features (Fig. 2B). This was confirmed by the depiction of the putative COOH-terminal α-helix (amino acids 56 to 77) as a helical wheel, giving a view of a helix from a protein sequence looking down the axis of the helix (Fig. 2C).

To delineate what regions of the GCP-2/CXCL6 molecule are responsible for antibacterial activity, a 50-amino-acid peptide of the NH₂-terminal region (GPV-50) of GCP-2/CXCL6 and a 19-amino-acid peptide (APF-19) corresponding to the putative amphipathic α-helix of the COOH-terminal region were compared with the GCP-2/CXCL6 holopeptide with regard to biochemical properties and antibacterial activity (Table

FIG. 2. Predicted structure of GCP-2/CXCL6 in relation to antibacterial activity. (A) Predictive model based on known structures of other members of the chemokine family. The NH$_2$ terminus, most likely, is an unstructured region followed by three antiparallel β-sheets that are held together by disulfide bonds involving the cysteines of the CXC motif (yellow). The COOH terminus is presumably an α-helix (purple). (B) The putative COOH-terminal α-helix (amino acids 56 to 77) has an amphipathic structure where hydrophobic (blue) and hydrophilic (white/yellow) amino acids are arranged in a polarized fashion. (C) The amphipathic character of the COOH terminus is further elucidated by depicting it as a helical wheel, giving a view of a helix from a protein sequence, looking down the axis of the helix.

2). We hypothesized that the COOH-terminal region could possess high antibacterial activity, since the amphipathic α-helical structure is a common feature of antibacterial peptides (2). The antibacterial activities of the peptide derivatives against *S. pyogenes* and *E. coli* were investigated using the bactericidal assay. Interestingly, GPV-50 clearly showed higher antibacterial activity than APF-19, but both peptides showed less antibacterial effect than the holopeptide (Tables 1 and 2).

**Effects of GCP-2/CXCL6 and its derivatives on liposomes.** Liposome leakage experiments were performed in order to investigate the correlation between bacterial killing and defect formation in lipid membranes and to further confirm our microscopy-based results showing bacterial membrane integrity compromise. Clear differences were observed between the peptide and its derivatives with regard to leakage induction. The holopeptide GCP-2/CXCL6 and the NH$_2$-terminal peptide GPV-50 showed comparable potency regarding leakage induction in negatively charged DOPE/DOPG liposomes. Their activities were comparable to the benchmark membrane-disruptive peptide LL-37, and they were considerably more potent than APF-19 (Fig. 3A). In the presence of 150 mM NaCl, liposome disruption decreased for all peptides investigated, suggesting that electrostatics plays a key role in the action of these compounds and corroborating numerous pre-

vious findings on antimicrobial peptides (Fig. 3B). The ranking of the peptides regarding leakage induction in liposomes and the effects of electrolytes on peptide-induced liposome disruption both correlate well with our results for bacterial killing, suggesting a pivotal role of the disruption of the lipid membrane(s) in the bacterial walls as a key component in the antibacterial action of these peptides. This notion is also corroborated by the rapid kinetics of liposome rupture: 70 to 80% of the leakage is reached after <1,000 s for APF-19 and GPV-50 (Fig. 3C). Quantitatively, liposome disruption by GCP-2/CXCL6 was markedly slower than that by GPV-50 and APF-19, reflecting slower diffusion to the liposome surface due to its larger size, but possibly also a more complex lipid membrane interaction.

**Helical content of GCP-2/CXCL6 and its derivatives as studied by CD spectroscopy.** In order to provide an experimental comparison to the molecular modeling prediction, CD measurements were performed. The results are shown in Table 3 and Fig. 4. In partial agreement with the modeling, both the peptide derivatives indeed display a certain degree of α-helical conformation, although helix formation is incomplete for each of these peptides, and for GPV-50 it is relatively minor in quantitative terms. For GCP-2/CXCL6, on the other hand, the total helical content is relatively great. Interestingly, the CD

TABLE 2. Biochemical properties and antibacterial activities of the holopeptide GCP-2/CXCL6 and its synthetic derivatives GPV-50 and APF-19[a] against the indicated bacteria

| Peptide | Molecular mass (kDa) | pI | No. of amino acid residues that are: | | | | MBC (μM)[b] for: | | | |
|---|---|---|---|---|---|---|---|---|---|---|
| | | | | | | | *S. pyogenes* | | *E. coli* | |
| | | | Hydrophobic | Hydrophilic | Positive | Negative | 50% | 90% | 50% | 90% |
| GCP-2 | 7.9 | 9.75 | 26 | 34 | 13 | 5 | 0.063 ± 0.01 | 0.30 ± 0.12 | 0.24 ± 0.03 | 0.46 ± 0.01 |
| GPV-50 | 5.3 | 9.75 | 18 | 20 | 7 | 2 | 0.4 ± 0.1 | 0.9 ± 0.02 | 0.8 ± 0.04 | 7.9 ± 0.2 |
| APF-19 | 2.1 | 10.2 | 6 | 10 | 5 | 1 | 5.7 ± 0.1 | 9.5 ± 0.1 | 5.6 ± 0.03 | 9.5 ± 0.05 |

[a] GPV-50 corresponds to the NH$_2$-terminal region of GCP-2/CXCL6, and APF-19 corresponds to its COOH-terminal region.
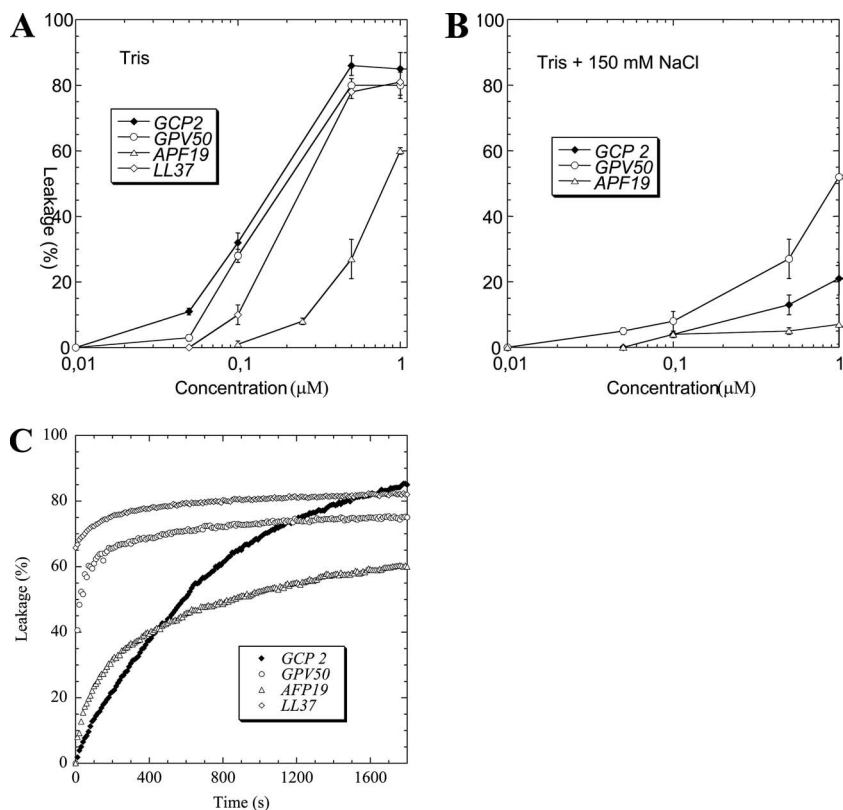[b] Values are means ± SEM.

FIG. 3. GCP-2/CXCL6 and its derivatives GPV-50 and APF-19 cause liposome leakage by membrane disruption. (A and B) CF-loaded liposomes were incubated with the holopeptide or one of its derivatives at the indicated concentrations in buffer alone (A) or buffer containing 150 mM NaCl (B). Leakage was determined by monitoring the fluorescence emitted at 520 nm and was expressed as a percentage of the leakage induced by Triton X-100, taken as 100%. Measurements were performed at 37°C. (C) The kinetics of leakage induction by the peptides was assessed, and results are shown.

measurements further show that the holopeptide and APF-19 underwent helix induction upon binding to anionic liposomes. In contrast, significant ordered-structure formation is observed upon binding of all three peptides to LPS, although it is not possible from the current data to determine whether the latter effects are due to peptide-induced conformational changes in LPS, LPS-induced conformational changes in the peptides, or both.

**Effects of NaCl and plasma on the antibacterial activity of GCP-2/CXCL6.** Many antibacterial peptides, such as defensins, show decreased activity in the presence of NaCl and plasma (9). To investigate whether the decreased liposomal leakage induced by the peptides in the presence of NaCl would also

TABLE 3. Helix contents of GCP-2/CXCL6 and its derivatives as measured by CD in the presence and absence of negatively charged liposomes

| Peptide | % Helix content in: | |
| --- | --- | --- |
| | Buffer alone | Buffer with DOPG/ DOPE liposomes |
| GCP-2 | 25 ± 5 | 23 ± 5 |
| GPV-50 | 17 ± 3 | 6 ± 3 |
| APF-19 | 13 ± 4 | 28 ± 5 |
| LL-37 | 25 ± 6 | 57 ± 5 |

influence bacterial killing, the bactericidal assay was used. Also, because the presence of plasma is known to inhibit the antibacterial activities of other peptides, we tested its influence on GCP-2/CXCL6-mediated killing. Since plasma alone affected the survival of *S. pyogenes* (7), strains of *S. aureus* (5120) and *E. coli* were chosen for investigation of the effect of plasma on antibacterial activity (Fig. 5). The presence of low concentrations of plasma strongly inhibited the killing of *S. aureus* by GCP-2/CXCL6, while plasma concentrations of 10% or higher were required to decrease the extent of killing of *E. coli* (Fig. 5A). A possible explanation for the difference in sensitivity to GCP-2/CXCL6-induced killing in the presence of plasma may be plasma protein-binding structures on the surface of *S. aureus*, providing protection against antibacterial peptides.

*S. pyogenes* and, to some extent, *E. coli* show decreased viability in the presence of NaCl at 150 mM. Therefore, *S. aureus* was chosen for examination of the effect of NaCl on the antibacterial activity of GCP-2/CXCL6 (Fig. 5B). Antibacterial activity was slightly reduced at 50 mM NaCl, while at 100 mM and 150 mM, most of the antibacterial activity was abolished.

It was not clear from the viable-count experiment and our microscopy findings whether, in the presence of NaCl, the binding of GCP-2/CXCL6 to bacteria is inhibited or whether the chemokine binds to the bacterial surface without affecting bacterial viability. Therefore, *S. aureus* (strain Newman) was
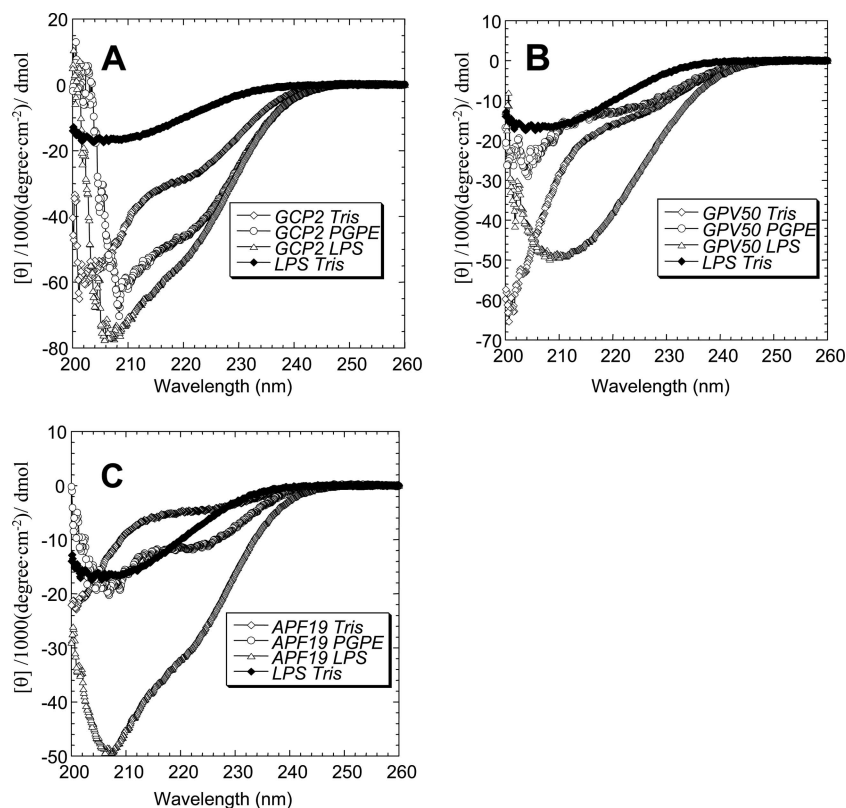
FIG. 4. Extent of helix formation of GCP-2/CXCL6 and its derivatives as studied by CD spectroscopy. Measurements were performed using a peptide concentration of 10 μM in buffer with or without the addition of liposomes or LPS as indicated. The helix content was quantified at a wavelength of 222 to 225 nm and 37°C. (A) GCP-2/CXCL6; (B) GPV-50; (C) APF-19.

incubated with GCP-2/CXCL6 in the presence or absence of 150 mM NaCl, followed by Western blot analysis of cell extracts using anti-GCP-2/CXCL6 antibodies. This revealed that in the absence of NaCl there was a strong GCP-2/CXCL6 signal, while in the presence of NaCl there was only a very weak signal (Fig. 5C). The weak signals in both samples at approximately 50 kDa most likely represent direct binding of primary and secondary antibodies to cell wall-anchored protein A. In contrast, protein A-mediated IgG binding to the bacteria, examined using peroxidase-labeled protein G, did not differ between samples incubated with or without NaCl. These results indicate that 150 mM NaCl directly inhibits the binding of GCP-2/CXCL6 to *S. aureus* and thereby inhibits the antibacterial activity of the peptide in vitro.

**The related chemokines ENA-78/CXCL5 and NAP-2/CXCL7 exert lower antibacterial activities than GCP-2/CXCL6.** The amino acid sequences of mature GCP-2/CXCL6, ENA-78/CXCL5, and NAP-2/CXCL7 were compared to each other. On the amino acid level, ENA-78/CXCL5 showed 78% similarity with GCP-2/CXCL6 while NAP-2/CXCL7 showed 18% similarity (data not shown). The antibacterial activities of ENA-78/CXCL5 and NAP-2/CXCL7 against *S. pyogenes* were compared with that of GCP-2/CXCL6 by using the bactericidal assay. ENA-78/CXCL5 and NAP-2/CXCL7 showed equally potent antibacterial activities against *S. pyogenes*; both were approximately 90-fold less active than GCP-2/CXCL6 (Table 4).

## DISCUSSION

This study shows for the first time that GCP-2/CXCL6 has antibacterial activity against several gram-positive and gram-negative aerobic bacteria relevant to mucosal and dermal infections. Our findings demonstrate a NaCl-sensitive binding of the peptide to the bacterial surface, resulting in membrane protrusions, bacterial killing, and, in parallel, an ability to induce liposomal leakage. The typical antimicrobial peptide is amphipathic and carries a positive net charge at physiological pH. It is believed to function via insertion into and disruption of the bacterial membrane or to act via intracellular targeting (2). GCP-2/CXCL6 is cationic, having a pI of 9.75. It also has amphipathic sequences, especially in its COOH-terminal region. There are structural similarities between GCP-2/CXCL6 and antibacterial defensins. The defensins are divided into two main groups: α and β. The α-defensins are produced in myeloid precursor cells in the bone marrow and stored in granules, while β-defensins are produced by epithelial cells and leukocytes (8). Like GCP-2/CXCL6, α-defensin-1 and -2 contain a conserved CXC motif in the NH₂-terminal region of the mature peptide, as do the structurally related β-defensins. These molecules, like GCP-2/CXCL6, have been shown to be chemotactic for leukocytes (3, 25). In addition, the antibacterial activities of both β-defensins and GCP-2/CXCL6 are sensitive to and inhibited by presence of NaCl at physiological concentrations. In summary, GCP-2/CXCL6 shares both structural
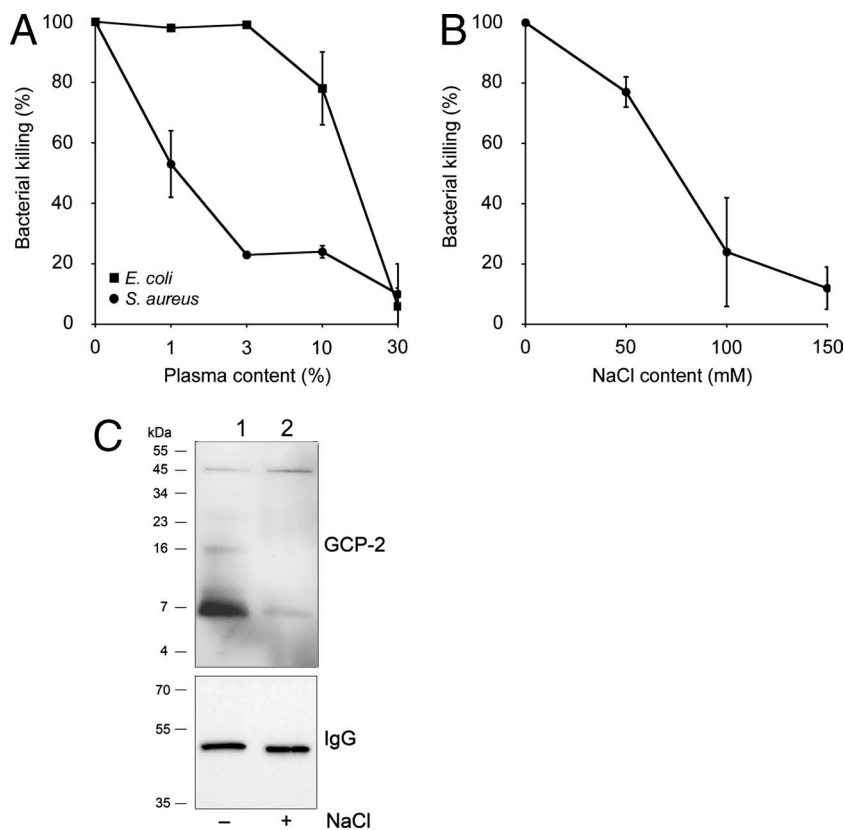
FIG. 5. Effects of plasma and NaCl on the antibacterial activity of GCP-2/CXCL6, investigated by using a bactericidal assay (peptide concentration, 1 μM for 1 h at 37°C). (A) The presence of plasma at low concentrations strongly inhibited the killing of *S. aureus*, while plasma concentrations of 10% or higher were required to decrease the killing of *E. coli*. (B) *S. aureus* was chosen for examination of the effect of NaCl on the antibacterial activity of GCP-2/CXCL6. The antibacterial activity in this setup was greatly reduced in the presence of 100 and 150 mM NaCl. Data are means from three separate experiments. Error bars, standard errors of the means. (C) The ability of GCP-2/CXCL6 to interact with the bacterial membrane in the absence (lane 1) and presence (lane 2) of 150 mM NaCl was investigated. GCP-2/CXCL6 or IgG was adsorbed to *S. aureus* in the presence or absence of NaCl as indicated, followed by SDS-PAGE separation and Western blot analysis using anti-GCP-2 antibodies or protein G, respectively. Molecular mass is indicated on the left.

and functional characteristics with defensins. Interestingly, our structural prediction of the intramolecular positioning of the antibacterial activity was not in accordance with the results from the CD spectroscopy studies. Indeed, both derivatives possessed helical contents, but GPV-50 was the more potent as a bactericidal agent. The lack of activity on *Candida albicans* may indicate a GCP-2/CXCL6 preference for non-ergosterol-containing membranes. The protrusions and leakage of intracellular material visualized by electron microscopy suggest a

peptide-mediated effect on the bacterial membrane, although the timing of this event cannot be precisely determined.

Expression of GCP-2/CXCL2 is induced mainly by inflammatory stimuli, such as IL-1β, at epithelial surfaces (28). Recently, we showed that inflamed pharyngeal epithelial cells possess an antibacterial activity that is, at least in part, dependent on expression of the interferon-dependent CXC chemokine MIG/CXCL9 (5). It must be considered that when relevant concentrations of IL-1β are generated, GCP-2/CXCL6 is likely to contribute to antimicrobial activity at the host-pathogen interface. In health, GCP-2/CXCL6 may, together with other regulators, contribute to maintaining a low but constant level of protection against bacterial colonization. By using LL-37 as a model peptide, the extent of α-helicity was shown to correlate with antibacterial activity against both gram-positive and gram-negative bacteria (13). The presence of NaCl alters peptide helicity and thus decreases antibacterial activity. The results from liposomal leakage studies and the bactericidal assay presented in the current study confirm that leakage induction and bacterial killing were negatively influenced by the presence of NaCl. Hence, it seems likely that GCP-2/CXCL6 exerts antibacterial activity in environments where NaCl and

TABLE 4. Comparison of antibacterial activities of the related ELR-positive CXC chemokines ENA–78/CXCL5 and NAP–2/CXCL7 using the bactericidal assay and *S. pyogenes*

| Chemokine | MBC (μM)[a] | |
|---|---|---|
| | 50% | 90% |
| GCP-2/CXCL6 | 0.063 ± 0.01 | 0.30 ± 0.12 |
| ENA-78/CXCL5 | 5.75 ± 1.9 | >10 |
| NAP-2/CXCL7 | 5.52 ± 1.8 | >10.5 |

[a] Values are means ± SEM from three separate experiments.

plasma levels are low. Such locales may include, for example, the mucosal surfaces of the oral cavity, tonsils, and the epithelial lining of the airways. The activity was highest against *S. pyogenes* and *S. dysgalactiae* subsp. *equisimilis*, two causative agents of tonsillitis. Possibly the tonsils are a locale displaying near-optimal conditions for the antibacterial activity of GCP-2/CXCL6. In addition, with regard to timing of the bacterial presence, an antibacterial peptide such as GCP-2/CXCL6 may exert its action in the initial phase of the encounter, prior to the efflux of plasma proteins and neutrophils to the site of injury. At later time points, plasma proteins will exert actions to restore homeostasis, and bacterial corruption of plasma proteins will have started.

Chemokines in general oligomerize and have glucosaminoglycan-binding properties. As a consequence, an accumulation on the surfaces of epithelial cells may provide an immobilized antibacterial gradient (19). Future studies will test this hypothesis. However, in order for an interaction between GCP-2/CXCL6 and the bacterial membrane to occur, a higher affinity than that between a glucosaminoglycan and a peptide may be required. Our CD spectroscopy data indicate that the holopeptide and the COOH-terminal peptide adopted a helical conformation upon interaction with either negatively charged liposomes or LPS. These findings provide new information on how this chemokine acts in its physiological setting upon the encounter with a bacterium, and perhaps such an environment-dependent conformational change can account for an anchoring mechanism. In a recent publication, Sumby et al. demonstrate the proteolytic degradation of GCP-2/CXCL6 and GRO-α/CXCL-1 by the streptococcal enzyme SpyCEP (24). This may serve as additional evidence that it is important to pathogenic bacteria to evade not only the neutrophil recruitment caused by GCP-2/CXCL6 but also its antibacterial activity.

In a previous study, GCP-2/CXCL6 was reported not to possess antibacterial activity (29). The protocols of the previous study and the current work differed. The presence of Trypticase soy broth in the bactericidal assay (which was used in the previous but not the current study) may have neutralized the antibacterial activity of GCP-2/CXCL6. In the current study, we also examined the related chemokines ENA-78/CXCL5 and NAP-2/CXCL7 for antibacterial activity. The primary amino acid sequence of human GCP-2/CXCL6 has a rather weak similarity with that of the related ELR-positive CXC chemokine IL-8/CXCL8 (30%), which is more homologous with ENA-78/CXCL5 (77%). Although ENA-78/CXCL5 showed 88% similarity and NAP-2/CXCL7 showed 64% similarity to GCP-2/CXCL6, these chemokines displayed low degrees of antibacterial activity in our hands. Interestingly, a COOH-terminal deletion product of NAP-2/CXCL7 isolated from human platelets has previously been reported to have direct antibacterial activity (14). Possibly such a COOH-terminal trimming is required for antibacterial activity, since we failed to record a potent activity for this peptide in our study. Perhaps a similar trimming of GCP-2/CXCL6, if this phenomenon occurs in vivo, would enhance its antibacterial effect.

In the future, GCP-2/CXCL6 and molecules derived from it may have a potential use as bactericidal agents. Exact mapping of the molecules' antibacterial activity and interaction with receptors is important, because receptor activation could lead to extensive inflammation through recruitment and activation of neutrophils. As a promoter of angiogenesis, a relevant derivative of GCP-2/CXCL6 could be of additional value in wound healing. Although further studies will be needed to address these applications, the discovery of the antibacterial activity of GCP-2/CXCL6 adds to our current understanding of the function of human innate defense peptides and the structural basis of their antibacterial activity.

## REFERENCES

1. **Baggiolini, M.** 2001. Chemokines in pathology and medicine. J. Intern. Med. **250:**91–104.
2. **Boman, H. G.** 2003. Antibacterial peptides: basic facts and emerging concepts. J. Intern. Med. **254:**197–215.
3. **Chertov, O., D. F. Michiel, L. Xu, J. M. Wang, K. Tani, W. J. Murphy, D. L. Longo, D. D. Taub, and J. J. Oppenheim.** 1996. Identification of defensin-1, defensin-2, and CAP37/azurocidin as T-cell chemoattractant proteins released from interleukin-8-stimulated neutrophils. J. Biol. Chem. **271:**2935–2940.
4. **Cole, A. M., T. Ganz, A. M. Liese, M. D. Burdick, L. Liu, and R. M. Strieter.** 2001. IFN-inducible ELR-CXC chemokines display defensin-like antimicrobial activity. J. Immunol. **167:**623–627.
5. **Egesten, A., M. Eliasson, H. M. Johansson, A. I. Olin, M. Mörgelin, A. Mueller, J. E. Pease, I. M. Frick, and L. Björck.** 2007. The CXC chemokine MIG/CXCL9 is important in innate immunity against *Streptococcus pyogenes*. J. Infect. Dis. **195:**684–693.
6. **Fillmore, R. A., S. E. Nelson, R. N. Lausch, and J. E. Oakes.** 2003. Differential regulation of ENA-78 and GCP-2 gene expression in human corneal keratocytes and epithelial cells. Investig. Ophthalmol. Vis. Sci. **44:**3432–3437.
7. **Frick, I. M., P. Åkesson, H. Herwald, M. Mörgelin, M. Malmsten, D. K. Nägler, and L. Björck.** 2006. The contact system—a novel branch of innate immunity generating antibacterial peptides. EMBO J. **25:**5569–5578.
8. **Ganz, T.** 2001. Antimicrobial proteins and peptides in host defense. Semin. Respir. Infect. **16:**4–10.
9. **Ganz, T.** 2003. Defensins: antimicrobial peptides of innate immunity. Nat. Rev. Immunol. **3:**710–720.
10. **Gijsbers, K., M. Gouwy, S. Struyf, A. Wuyts, P. Proost, G. Opdenakker, F. Penninckx, N. Ectors, K. Geboes, and J. Van Damme.** 2005. GCP-2/CXCL6 synergizes with other endothelial cell-derived chemokines in neutrophil mobilization and is associated with angiogenesis in gastrointestinal tumors. Exp. Cell Res. **303:**331–342.
11. **Hieshima, K., H. Ohtani, M. Shibano, D. Izawa, T. Nakayama, Y. Kawasaki, F. Shiba, M. Shiota, F. Katou, T. Saito, and O. Yoshie.** 2003. CCL28 has dual roles in mucosal immunity as a chemokine with broad-spectrum antimicrobial activity. J. Immunol. **170:**1452–1461.
12. **Humphrey, W., A. Dalke, and K. Schulten.** 1996. VMD: visual molecular dynamics. J. Mol. Graph. **14:**33–38.
13. **Johansson, J., G. H. Gudmundsson, M. E. Rottenberg, K. D. Berndt, and B. Agerberth.** 1998. Conformation-dependent antibacterial activity of the naturally occurring human peptide LL-37. J. Biol. Chem. **273:**3718–3724.
14. **Krijgsveld, J., S. A. Zaat, J. Meeldijk, P. A. van Veelen, G. Fang, B. Poolman, E. Brandt, J. E. Ehlert, A. J. Kuijpers, G. H. Engbers, J. Feijen, and J. Dankert.** 2000. Thrombocidins, microbicidal proteins from human blood platelets, are C-terminal deletion products of CXC chemokines. J. Biol. Chem. **275:**20374–20381.
15. **Maheshwari, A., R. D. Christensen, and D. A. Calhoun.** 2003. ELR$^+$ CXC chemokines in human milk. Cytokine **24:**91–102.
16. **Mine, S., K. Nasu, J. Fukuda, B. Sun, and I. Miyakawa.** 2003. Secretion of granulocyte chemotactic protein-2 by cultured human endometrial stromal cells. Fertil. Steril. **79:**146–150.

17. **Prause, O., M. Laan, J. Lotvall, and A. Linden.** 2003. Pharmacological modulation of interleukin-17-induced GCP-2-, GRO-α- and interleukin-8 release in human bronchial epithelial cells. Eur. J. Pharmacol. **462:**193–198.

18. **Proost, P., C. De Wolf-Peeters, R. Conings, G. Opdenakker, A. Billiau, and J. Van Damme.** 1993. Identification of a novel granulocyte chemotactic protein (GCP-2) from human tumor cells. In vitro and in vivo comparison with natural forms of GRO, IP-10, and IL-8. J. Immunol. **150:**1000–1010.

19. **Proudfoot, A. E.** 2006. The biological relevance of chemokine-proteoglycan interactions. Biochem. Soc. Trans. **34:**422–426.

20. **Rice, P., I. Longden, and A. Bleasby.** 2000. EMBOSS: the European Molecular Biology Open Software Suite. Trends Genet. **16:**276–277.

21. **Roth, J., M. Bendayan, and L. Orci.** 1978. Ultrastructural localization of intracellular antigens by the use of protein A-gold complex. J. Histochem. Cytochem. **26:**1074–1081.

22. **Sachse, F., F. Ahlers, W. Stoll, and C. Rudack.** 2005. Neutrophil chemokines in epithelial inflammatory processes of human tonsils. Clin. Exp. Immunol. **140:**293–300.

23. **Schwede, T., J. Kopp, N. Guex, and M. C. Peitsch.** 2003. SWISS-MODEL: an automated protein homology-modeling server. Nucleic Acids Res. **31:**3381–3385.

24. **Sumby, P., S. Zhang, A. R. Whitney, F. Falugi, G. Grandi, E. A. Graviss, F. R. Deleo, and J. M. Musser.** 2008. A chemokine-degrading extracellular protease made by group A *Streptococcus* alters pathogenesis by enhancing evasion of the innate immune response. Infect. Immun. **76:**978–985.

25. **Territo, M. C., T. Ganz, M. E. Selsted, and R. Lehrer.** 1989. Monocyte-chemotactic activity of defensins from human neutrophils. J. Clin. Investig. **84:**2017–2020.

26. **Wolf, M., M. B. Delgado, S. A. Jones, B. Dewald, I. Clark-Lewis, and M. Baggiolini.** 1998. Granulocyte chemotactic protein 2 acts via both IL-8 receptors, CXCR1 and CXCR2. Eur. J. Immunol. **28:**164–170.

27. **Wuyts, A., P. Proost, J. P. Lenaerts, A. Ben-Baruch, J. Van Damme, and J. M. Wang.** 1998. Differential usage of the CXC chemokine receptors 1 and 2 by interleukin-8, granulocyte chemotactic protein-2 and epithelial-cell-derived neutrophil attractant-78. Eur. J. Biochem. **255:**67–73.

28. **Wuyts, A., S. Struyf, K. Gijsbers, E. Schutyser, W. Put, R. Conings, J. P. Lenaerts, K. Geboes, G. Opdenakker, P. Menten, P. Proost, and J. Van Damme.** 2003. The CXC chemokine GCP-2/CXCL6 is predominantly induced in mesenchymal cells by interleukin-1β and is down-regulated by interferon-gamma: comparison with interleukin-8/CXCL8. Lab. Investig. **83:**23–34.

29. **Yang, D., Q. Chen, D. M. Hoover, P. Staley, K. D. Tucker, J. Lubkowski, and J. J. Oppenheim.** 2003. Many chemokines including CCL20/MIP-3α display antimicrobial activity. J. Leukoc. Biol. **74:**448–455.